M&C 2017 - International Conference on Mathematics & Computational Methods Applied to Nuclear Science & Engineering, Jeju, Korea, April 16-20, 2017, on USB (2017)

Impact of Fuel Behaviour Uncertainties on UAM-LWR TMI-1 Pin Cell Case

A. Taavitsainen, R. Vanhanen, T. Ikonen[†], V. Valtavirta[†]

[†]*VTT Technical Research Centre of Finland Ltd., P.O. Box 1000, FI-02044, VTT, Finland*
aapo.taavitsainen@gmail.com, risto.vanhanen@iki.fi, timo.ikonen@iki.fi

Abstract - *Uncertainty Analysis in Modelling (UAM) benchmark initiated by the OECD/NEA focuses on studying the propagation of uncertainties in the modelling of Light Water Reactors (LWRs). Its Phase I pin cell exercises consider multi-group microscopic cross section uncertainties. The objective of the present study is to include fuel behaviour uncertainties into the benchmark framework and determine their relative importance on the total neutronics output uncertainty. The output uncertainty has been propagated statistically from the input uncertainties by applying statistically perturbed input parameters to fuel behaviour code FINIX and deterministic lattice code DRAGON. Results are presented for two neutronics output parameters. The study has been performed for the TMI-1 test case of the UAM benchmark's cell physics exercise I-1.*

I. INTRODUCTION

Nuclear data and nuclear fuel behaviour parameters are, in part, used as input data in the modelling of nuclear reactors. Alas, due to measurement inaccuracies, imperfections in fuel fabrication, and lack of knowledge related to certain phenomena, uncertainties in the input parameters and certain models cannot be completely eliminated. Therefore, the output of a best estimate model is also uncertain. The epistemic uncertainty of the model output can be estimated, e.g., with stochastic uncertainty analysis in which a best estimate model is repeatedly evaluated with statistically perturbed input data. This yields, given uncertainty distributions (i.e., distributions that describe the uncertainties) of the input parameters, uncertainty distributions of the output parameters. It is also possible to identify the major sources of the uncertainty with sensitivity analysis.

The cell physics Exercise I-1 TMI-1 PWR of the OECD/NEA UAM-LWR (Uncertainty Analysis in Modelling for Design, Operation and Safety Analysis of LWRs) benchmark [1] studies the output neutronics uncertainties due to only the nuclear data uncertainties in a pin cell case of the Three Mile Island Pressure Water Reactor. In this work, we will extend the benchmark case by considering its multiphysics aspects. The uncertainties in the nuclear data, fuel fabrication, and fuel behaviour models are accounted for.

More specifically, the original benchmark considers microscopic neutron cross sections $\sigma(E)$, fission neutron yields $\nu(E)$, and fission spectra $\chi(E, E')$ for each nuclide as the sources of the input uncertainty. For simplicity, we account only for the cross section uncertainties. Additionally, material densities $\rho(T_i)$, geometry parameters such as fuel outer radii $r(T_i)$, and regional temperatures T_i are considered as uncertain. These are the input parameters for the neutronics calculations and the output parameters of the fuel behaviour calculations. The uncertain input parameters of the fuel behaviour calculations include fuel fabrication dimensions, thermal hydraulic boundary conditions, and model parameters. All these parameters are inherently positive.

In this work, the output uncertainty will be quantified with a novel statistical uncertainty analysis method called CFENSS–SRS (**C**oupled **F**uel B**e**haviour and **N**eutronics **S**tochastic **S**ampling with **S**imple **R**andom **S**ampling). The method was developed in the course of the study.

It is shown that the uncertainties originating from nuclear fuel behaviour can cause a 20 % to 70 % increase in the uncertainties of the neutronics output parameters. We also demonstrate that the use of a simple zero-cut-off method for handling sampled negative values of inherently positive parameters leads to skewed uncertainty distributions of the output parameters.

II. THEORY

Microscopic neutron cross sections are both nuclide and reaction-wise effective cross-sectional areas of a nucleus. They can be understood as inherently positive energy dependent continuous variables. In literature they are generally processed and condensed into discrete energy groups and, in statistical uncertainty propagation, the formed multigroup microscopic cross sections are perturbed with respective multigroup covariances [1,2]. This approach is valid for traditional deterministic neutronics codes. Alternatively, for stochastic Monte Carlo neutronics codes, the input uncertainties have been introduced to the continous energy microscropic cross sections [3,4].

Concerning the nuclear data perturbations, the CFENSS–SRS approach can be employed to introduce nuclear data uncertainties to both the deterministic and the Monte Carlo codes. Moreover, the approach accounts for nuclear fuel uncertainties which are an important source of uncertainty often neglected in the neutronics calculations. Here we shall cover the main theory of the CFENSS–SRS method while a more detailed description can be found in Ref. [5].

In the CFENSS–SRS method the nuclear data of a nuclear data library is first processed into continuous energy format. The data remains unprocessed apart from a simple interpolation between the data points. Assuming a full within-group correlation a set of groupwise multiplicative perturbation factors P_g can be applied to the pointwise nuclear data:

$$\sigma_{g,\text{perturbed}} = P_g \cdot (\sigma_{\mathrm{E}_1}, ..., \sigma_{\mathrm{E}_n}) = (P_g\sigma_{\mathrm{E}_1}, ..., P_g\sigma_{\mathrm{E}_n}), \quad (1)$$

so that $(\mathrm{E}_1, ..., \mathrm{E}_n) \in [\tilde{E}_g, \tilde{E}_{g-1}]$. Here the perturbation formula is written for the cross sections although it applies also for other nuclear data. It is noted that possible summations rules

must be preserved during the perturbation step. The perturbation factors are based on the uncertainty data and introducing them in the early stage of the processing chain ensures that they will propagate through the whole nuclear data processing chain. Furthermore, this allows processing the perturbed data either into a continuous energy nuclear data library for the Monte Carlo codes or into a multigroup format for the deterministic lattice codes.

The perturbation factors are generated from the groupwise covariance data of the energy group averages available in evaluated nuclear data libraries. It is applied to respective multigroup best estimate cross sections to compute the perturbation factors via Simple Random Sampling. Generating uncorrelated perturbation factors requires, for example, a spectral decomposition [6] or a Cholesky-like decomposition [3] as the multigroup covariance data is generally correlated between the energy groups.

The nuclear data covariance matrices are not always valid covariance matrices as in some cases the data do not either meet the condition of positive-semidefinity or follow the summation rules in case of redundant covariance data. However, the data can be corrected, e.g., by computing the nearest symmetric positive-semidefinite covariance matrix in the sense of a weighted Frobenius norm [7]. It is also possible to find the nearest matrix that is consistent with the redundancies [8].

Similar to the nuclear data, the fuel behaviour uncertainties are reported as the best estimate and the variance of a parameter. The best estimate is typically taken to be the mean value of the uncertainty distribution. For simplicity, the parameters are often assumed as mutually independent and thus the covariance matrices reduce into a set of one-dimensional variances. [9] Therefore, acquiring their perturbation factors requires only the knowledge of a univariate distribution for drawing the samples with the uncertainty data being mathematically valid without further processing.

Following the Principle of Maximum Entropy [10, 11, 12, 13, 14] yields a truncated normal distribution as the Maximum Entropy Probability Distribution of an inherently positive parameter with prescribed mean and covariance [13, 15]. Alas, currently there exists no sampling method for even a one-dimensional arbitrary truncated normal distribution as, given the means and covariances, there exists no analytical or numerical method to compute the parameters of the distribution [5, 15]. With limited uncertainties ($\lesssim 60\,\%$) a normal distribution can be used as an approximation for the nuclear data while resampling the negative values. The univariate nuclear fuel parameters, in turn, can be sampled from the truncated normal distribution with a symmetric 2.5 % cut-off while approximating the distribution parameters with those of a normal distribution [9]. With limited uncertainties, both approximations are practical [5].

For simplicity, the sampling was performed with Simple Random Sampling as opposed to stratified sampling methods such as Latin Hypercube Sampling. A sufficient sample size was determined with a coverage approach based on tolerance intervals [16, 17, 18, 19]. For instance, for studying uncorrelated univariate parameters 93 samples is enough for reaching a two-sided one-dimensional tolerance interval with the probability of 95 % for the population coverage of 95 %.

III. CALCULATIONS

The calculations were performed in the framework of the TMI-1 hot full power pin cell exercise of the UAM benchmark and consider only fresh fuel. Deterministic lattice code DRAGON 5.0.1 [20] and fuel behaviour code FINIX 0.15.6 [21, 22] were used for the neutronics and fuel behaviour calculations, respectively. The codes were coupled using the fuel rod temperature, density, and geometry data from FINIX's output as the input of the DRAGON code. This allowed propagating the nuclear fuel input uncertainties to the neutronics calculation. The DRAGON code required a regionally homogeneous step temperature profile while FINIX applied a continuous linearly interpolated profile. Rowland's parabolic model was used to compute the effective homogeneous fuel temperature while the gas gap and the cladding temperatures were simply volume averaged due to a low neutron absorption [23]. EXCELT tracking module and SHI self-shielding module with Livolant-Jeanpierre model, Nordheim distributed model and Riemann integration method were used in the DRAGON calculations for a higher best estimate accuracy [20].

Of the nuclear data, only neutron cross section uncertainties were propagated. The evaluated neutron cross section covariance matrices were processed with a C++ code ECTS 0.93 beta (Evolved Covariance Tool Set) to reconstruct valid positive semidefinite covariance matrices. The code utilized a slightly modified NJOY2012.50 [24] to process the covariances into the groupwise format. The covariance data was obtained by supplementing relative covariance matrices from ENDF/B-VII.1 evaluation [25] with relative low-fidelity covariances [26] where no high-fidelity data were available. Thus, it was assumed that the relative covariances were generalizable for other evaluations with the low-fidelity covariances being gathered for the ENDF/B-VII.0 evaluation. The approach was based on Refs. [1, 27]. The perturbation step was performed with a Python code before processing the data into a slightly modified XMAS-172 [28] multigroup DRAGLIB format with an NJOY99.396 [29] extended with a DRAGR module used for converting the data to the DRAGLIB format used by DRAGON.

The CFENSS–SRS method can be applied also to the fission neutron yield $\nu(E)$ and the fission spectrum $\chi(E, E')$. In this study, however, they were accounted for by assuming the validity of a 42.5 % share of the total uncertainty 0.512 % contributed to the $\nu(E)$ and $\chi(E, E')$ of ^{235}U and ^{238}U in Ref. [30]. The neglected source of uncertainty was included by assuming the sources to be independent as described in the evaluated nuclear data.

The fuel behaviour uncertainties were adopted from Ref. [9]. The parameters with their mean values and the limits of the truncated normal distributions are listed in Tab. I. Materials properties such as thermal conductivity are described in FINIX as experimental correlations, for which only the uncertainty around the nominal value is given. The parameters were sampled with the Python code. It is notable that temperature uncertainties were not introduced directly but rather propagated by FINIX from the input uncertainties of Tab. I.

Parameter	BE $\pm\Delta$
Cladding outer diameter	(10.92 ± 0.06) mm
Cladding thickness	(0.673 ± 0.025) mm
Pellet outer diameter	(9.40 ± 0.02) mm
Fuel enrichment	(4.850 ± 0.003) atom $-$ %
Density (% of the theoretical)	(93.8 ± 1.6) %
Coolant pressure	(15.51 ± 0.31) MPa
Coolant inlet temperature	(561 ± 3) K
Coolant mass flux	(3460 ± 69) kg m^{-2} s^{-1}
Fuel thermal conductivity	± 10 %
Fuel thermal expansion	± 15 %
Cladding thermal conductivity	± 5 W m^{-1} K^{-1}
Cladding thermal expansion	± 30 %
Gas thermal conductivity	± 0.02 W m^{-1} K^{-1}
Coolant heat transfer	± 5 %

TABLE I: Perturbed fuel behaviour parameters with their nominal or best estimate (BE) values and one-dimensional uncertainties.

IV. RESULTS AND ANALYSIS

The results are divided into two parts: the primary results discuss the share of the nuclear fuel uncertainties in the neutronics calculations, while the secondary results consider the sampling distribution's impact on the shape of the response distribution. Two neutronics responses, namely the effective multiplication factor k_{eff} and $\nu\Sigma_{\text{f}}$, were studied. The responses are treated individually without considering any correlation between them.

1. Effect of Fuel Behaviour and Nuclear Data Uncertainties

The results of the uncertainty analysis are presented in Tabs. II and III. The results consist of three different sampling runs. The first and the second run considered solely the cross section or the fuel uncertainties, while the third run considered both the nuclear fuel parameters and the cross sections to be uncertain.

We shall first focus on the effective multiplication factor. The output uncertainty due to the cross sections is 0.390 % (run A) while the uncertainty due to the fuel parameters is 0.265 % (run B). Combining these two with the well-known summation in quadrature yields an uncertainty of 0.472 %. The value is well within the 95 % confidence interval of the corresponding sampled uncertainty of 0.484 % (run C). Therefore, it is plausible that the uncertainty contributions of the cross sections and the fuel parameters are not strongly dependent as the summation in quadrature applies for uncorrelated parameters.

It is also noted that all three sampled relative uncertainties are outside each other's confidence intervals, implying that the differences are likely the consequence of the perturbations and not due to chance alone. This is more clear from Fig. 1a. Including the nuclear fuel uncertainties increases the total uncertainty around 24 %.

Sources of uncertainty		n	$\bar{m}$	$\bar{v}_{\text{rel}}$ [%]
A) Cross sections	k_{eff}	411	1.410167	0.390
	$\nu\Sigma_{\text{f}}$		0.100 cm^{-1}	0.867
B) Fuel behaviour	k_{eff}	1000	1.408507	0.265
	$\nu\Sigma_{\text{f}}$		0.098 cm^{-1}	1.086
C) Fuel and cross sections	k_{eff}	407	1.408534	0.484
	$\nu\Sigma_{\text{f}}$		0.098 cm^{-1}	1.444

TABLE II: Sample sizes n, arithmetic means $\bar{m}$, and relative standard deviations $\bar{v}_{\text{rel}}$ for two neutronics output parameters with three different sources of uncertainty. The minimum sample size was set to be 93 samples based on the tolerance intervals while the final sample size was determined by the available computational resources.

Sources of uncertainty		p	$\Delta\bar{m}$	$\Delta\bar{v}_{\text{rel}}$ [%]
A) Cross sections	k_{eff}	0.40	53 pcm	0.365; 0.419
	$\nu\Sigma_{\text{f}}$	0.32	8.4E$-$5 cm^{-1}	0.811; 0.930
B) Fuel behaviour	k_{eff}	0.07	23 pcm	0.254; 0.277
	$\nu\Sigma_{\text{f}}$	0.18	6.6E$-$5 cm^{-1}	1.040; 1.135
C) Fuel and cross sections	k_{eff}	0.93	66 pcm	0.453; 0.520
	$\nu\Sigma_{\text{f}}$	0.87	1.4E$-$4 cm^{-1}	1.351; 1.550

TABLE III: Parametric 95 % confidence intervals for the arithmetic means and the relative standard deviations with their χ^2 normality test p-values.

Including the 42.5 % share of the neglected nuclear data uncertainty sources yields 0.485 % and 0.553 % as the propagated neutronics uncertainty due to nuclear data uncertainty, and the total combined uncertainty of nuclear fuel and nuclear data, respectively. The values can be compared to the values published for the UAM benchmark. The corresponding 95 % confidence intervals of the neutronics uncertainty and the total combined nuclear data and fuel uncertainty are now [0.454; 0.521] and [0.520; 0.590], respectively. The deterministic result of 0.512 % presented in Ref. [30] is within the interval for the nuclear data uncertainty.

The results for the $\nu\Sigma_{\text{f}}$ are 0.867 % (run A), 1.086 % (run B) and 1.444 % (run C). Similar to the k_{eff}, the total uncertainty of 1.390 % summed in quadrature from runs A and B is well within the 95 % confidence interval of the run C. The increase in the relative uncertainty is now 67 %. Also these results are outside each other's confidence intervals, as shown in Fig. 1b, which implies the differences to be statistically significant.

2. Shape of a Response Distribution

As a secondary result, it was shown that the shape of the output distribution depends quite strongly on the approximation of the input uncertainty distributions. The empirical

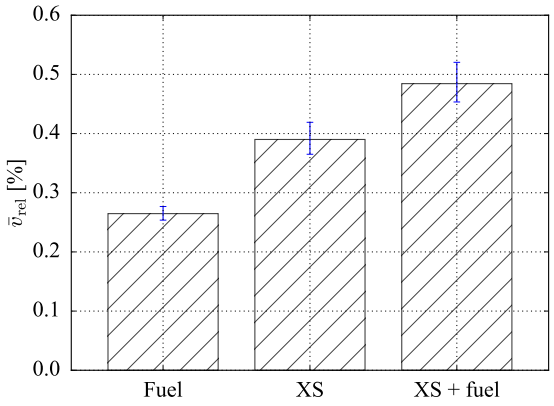

(a)

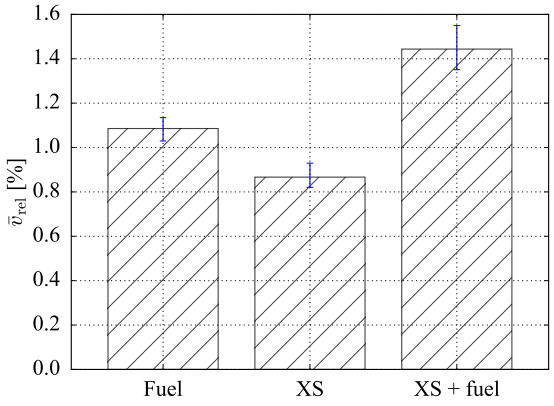

(b)

Fig. 1: Relative standard deviations for **(a)** k_{eff} and **(b)** $\nu\Sigma_{\mathrm{f}}$ with their 95 % confidence intervals. 'XS' refers to the cross sections as the source of the uncertainty.

cumulative distribution functions (ECDFs) of the k_{eff} for all three runs are presented in Fig. 2 alongside with the fitted CDFs of the normal distribution. The ECDFs visualize the data without additional distorting assumptions. The respective approximated probability distribution functions (PDF) are shown in Fig. 3. These are similar to the fitted PDFs as can be expected based on the p-values. Similar results for the $\nu\Sigma_{\mathrm{f}}$ are gathered in Figs. 4 and 5. The best estimate value of the run A differs from the runs B and C due to a slightly different temperature profile used in the neutronics calculations. Runs B and C used a temperature profile from the FINIX calculations while the run A used the temperature profile defined in the benchmark specifications.

The three samples are compared in Fig. 6 alongside with a fourth run applying a simple zero-cut-off method for removing the sampled negative values. The resampling of the negative values during the perturbation step yields approximately symmetrical distributions while the zero-cut-off method leads to a

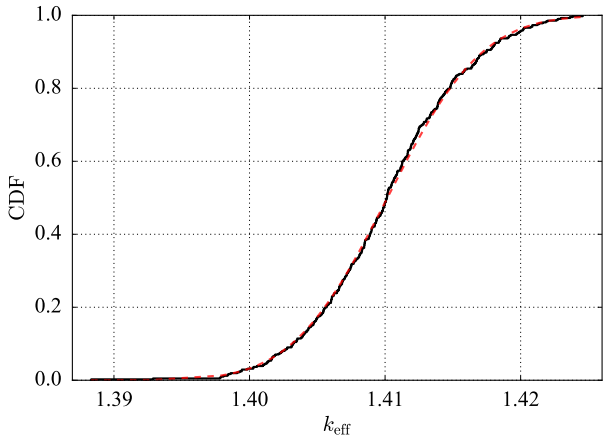

(a)

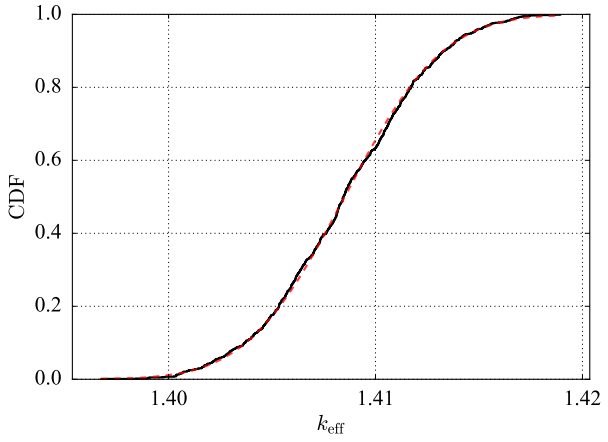

(b)

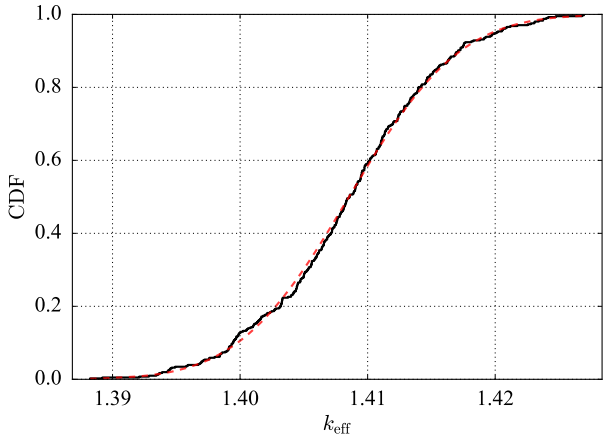

(c)

Fig. 2: Empirical cumulative distribution functions (solid black curves) of k_{eff} for runs **(a)** A, **(b)** B, and **(c)** C with their fitted normal distribution counterparts (dashed red curves).

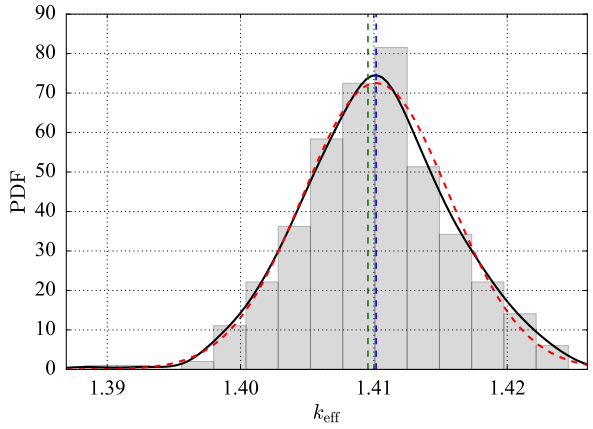

(a)

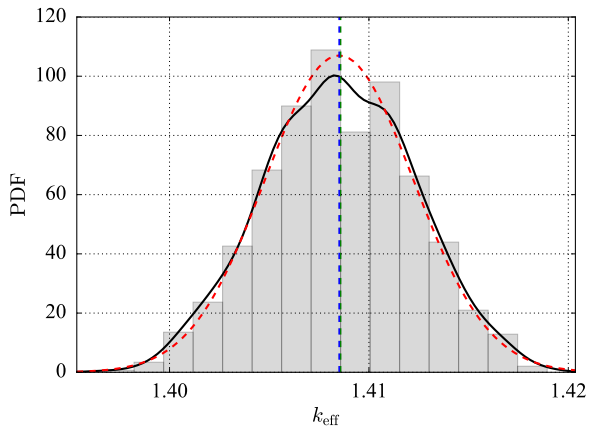

(b)

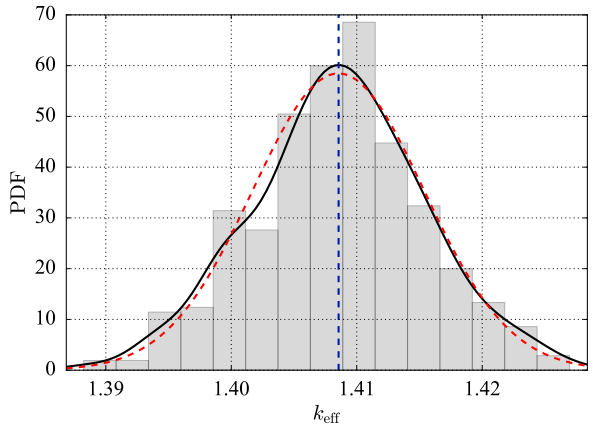

(c)

Fig. 3: Kernel density estimates of the probability distribution functions (solid black curves) of k_{eff} for runs **(a)** A, **(b)** B, and **(c)** C alongside with fitted normal distribution PDFs (dashed red curves). The green and blue dashed vertical lines mark unperturbed best estimate values and sample means, respectively.

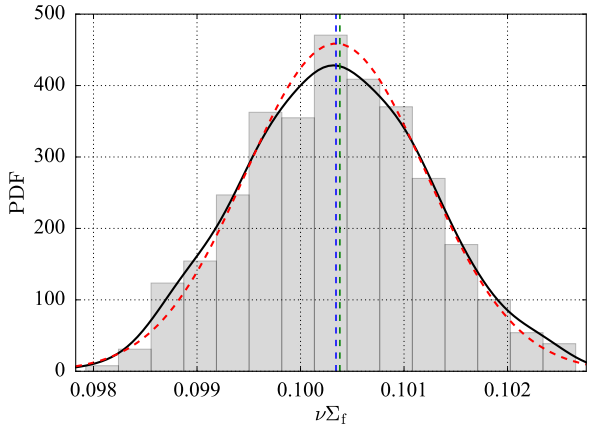

(a)

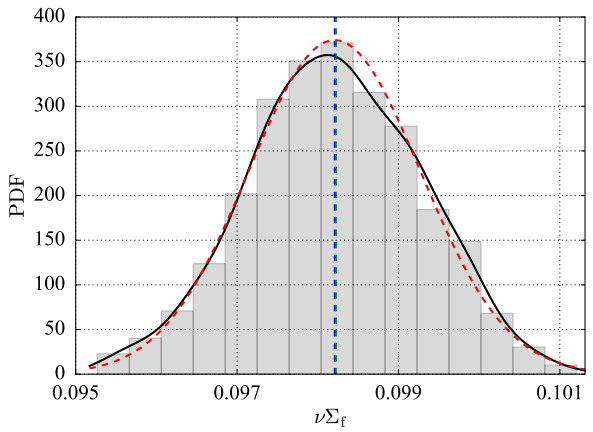

(b)

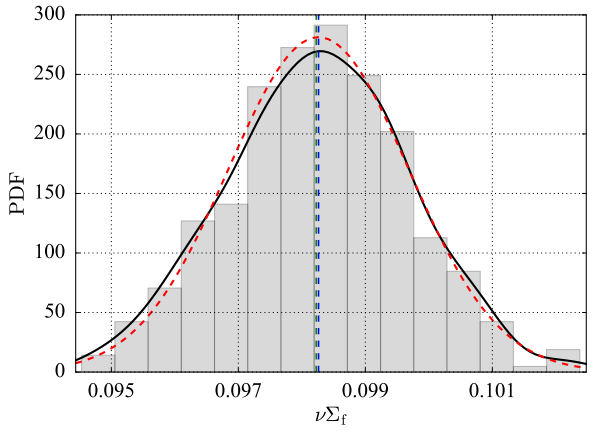

(c)

Fig. 4: Kernel density estimates of the probability distribution functions (solid black curves) of $\nu\Sigma_{\text{f}}$ for runs **(a)** A, **(b)** B, and **(c)** C alongside with fitted normal distribution PDFs (dashed red curves). The green and blue dashed vertical lines mark unperturbed best estimate values and sample means, respectively.

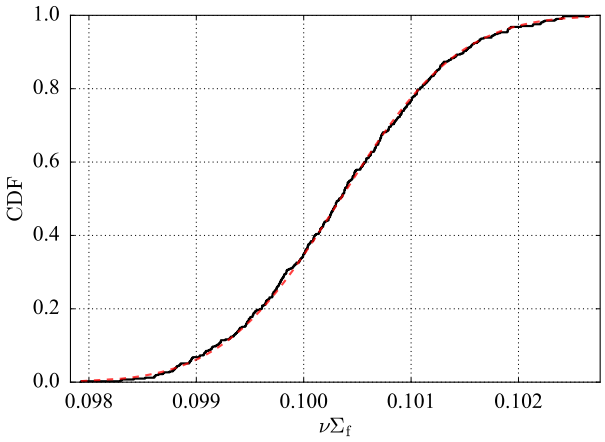

(a)

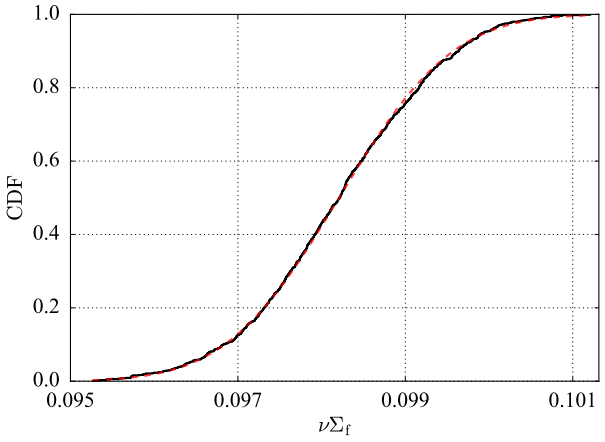

(b)

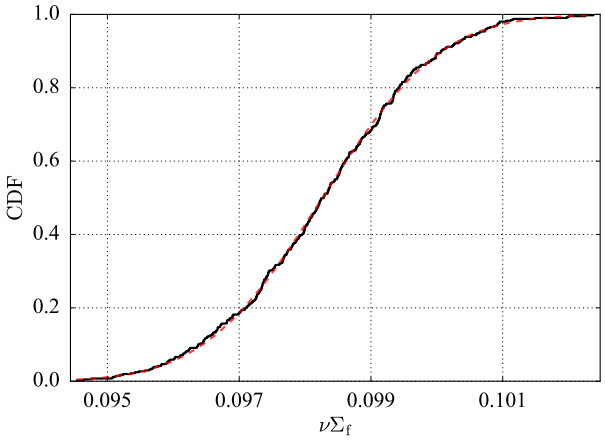

(c)

Fig. 5: Empirical cumulative distribution functions (solid black curves) of $\nu\Sigma_f$ for runs **(a)** A, **(b)** B, and **(c)** C with their fitted normal distribution counterparts (dashed red curves).

skewed distribution. The statistically non-significant p-values (> 0.05) of the χ^2 normality tests presented in Tab. III imply that there is no statistically significant deviation from a normal distribution. However, the actual output distribution can not be simulated using stochastic uncertainty analysis without a method to draw samples from general truncated normal distributions with a known mean and a covariance.

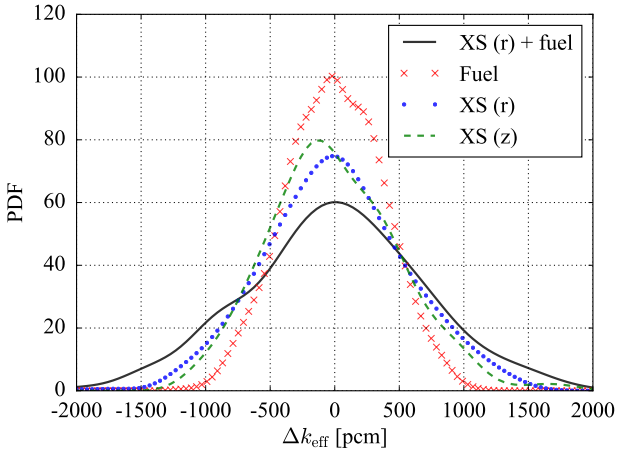

(a)

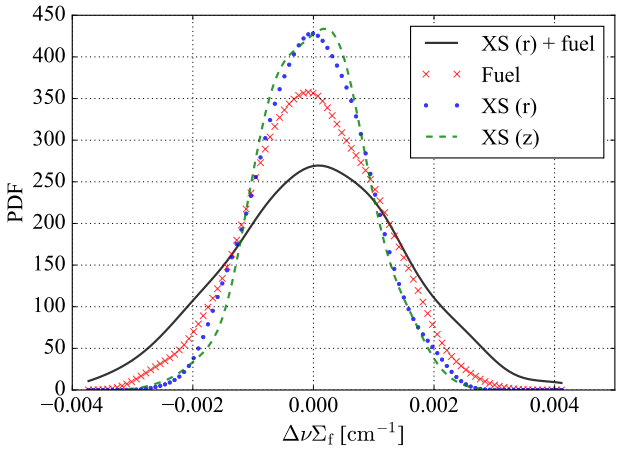

(b)

Fig. 6: Kernel density estimates (i.e., approximated probability distribution functions) of the samples presented in Tab. II for **(a)** k_{eff} and **(b)** $\nu\Sigma_f$. Keywords 'XS' and 'fuel' denote the source of the input uncertainty with the 'XS' referring to the microscopic cross sections. The method for handling the sampled negative cross section values is represented by 'r' or 'z' corresponding to the resampling of the negative values and the simple zero-cut-off approach, respectively. All three runs in Tabs. II and III applied the resampling approach.

V. CONCLUSIONS

Combined nuclear fuel and neutronics uncertainty analysis was performed on a TMI-1 pin cell case in the framework of the UAM benchmark. It was shown that accounting for the nuclear fuel uncertainties yields 24 % and 67 % higher relative output uncertainties for k_{eff} and $\nu\Sigma_{\text{f}}$, respectively. The fuel uncertainties should therefore be accounted for if the researcher wishes to present a significant second digit of the uncertainty value. Even though the uncertainties in the fission neutron yield and the fission spectrum were not considered here, the results indicate that the fuel behaviour uncertainties should be considered in multiphysics neutronics calculations. Although beyond the scope of the present work, the role of thermal hydraulic uncertainties may be speculated to have a similar importance.

Additionally, it was demonstrated that fuel behaviour and nuclear data uncertainties could be handled as independent sources of uncertainty at least with a reasonable accuracy. With larger sample sizes, it is likely that at least weak dependencies may be found.

It was also shown that the sampling method affects the shape of the output uncertainty distribution. Resampling of the negative values of inherently positive parameters leads to approximately symmetrical distributions while a crude zero-cut-off method yields skewed distributions.

It is noted that this study considered only one computational case of fresh fuel and two output neutronics parameters. Thus, the results should be confirmed in other reactor conditions and pin cell types before presenting more general conclusions.

VI. ACKNOWLEDGMENTS

The financial support of the SAFIR2018 programme is acknowledged. The CFENSS–SRS method was developed in the facilities of the Aalto University School of Science.

REFERENCES

1. K. IVANOV ET AL., "Benchmarks for Uncertainty Analysis in Modelling (UAM) for the Design, Operation and Safety Analysis of LWRs – Volume I: Specification and Support Data for Neutronics Cases (Phase I)," (2013), NEA/NSC/DOC(2013)7.
2. R. N. BRATTON, M. AVRAMOVA, and K. IVANOV, "OECD/NEA Benchmark for Uncertainty Analysis in Modelling (UAM) for LWRs – Summary and Discussion of Neutronics Cases (Phase I)," *Nuclear Engineering and Technology*, **46**, *3*, 313–342 (2014).
3. W. WIESELQUIST, T. ZHU, A. VASILIEV, and H. FERROUKHI, "PSI Methodologies for Nuclear Data Uncertainty Propagation with CASMO-5M and MCNPX: Results for OECD/NEA UAM Benchmark Phase I," *Science and Technology of Nuclear Installations*, **2013** (2013), Art. ID 549793, 15 pages.
4. T. ZHU, *Sampling-Based Nuclear Data Uncertainty Quantification for Continuous Energy Monte Carlo Codes*, Ph.D. thesis, École Polytechnique Fédérale de Lausanne (2015).
5. A. TAAVITSAINEN, *CFENSS–SRS method for the uncertainty analysis of nuclear fuel and neutronics*, Master's thesis, Aalto University School of Science (2016).
6. I. PANKA, A. KERESZTÚRI, and C. MARÁCZY, "Selected examples on multiphysics researches at KFKI AEKI – Results for Phase I of the OECD/NEA UAM benchmark," in "Proceedings of the Twentieth Symposium of Atomic Energy Research," (September 2010).
7. R. VANHANEN, "Computing Positive Semidefinite Multigroup Nuclear Data Covariances," *Nuclear Science and Engineering*, **179**, *4*, 411–422 (2015).
8. R. VANHANEN, "Computing More Consistent Multigroup Nuclear Data Covariances," *Nuclear Science and Engineering*, **181**, *1*, 60–71 (2015).
9. T. IKONEN and V. TULKKI, "The importance of input interactions in the uncertainty and sensitivity analysis of nuclear fuel behavior," *Nuclear Engineering and Design*, **275**, 229–241 (2014).
10. E. T. JAYNES, "Information Theory and Statistical Mechanics," *Physical Review*, **106**, *4*, 620–630 (1957).
11. E. T. JAYNES, "Prior Probabilities," *IEEE Transactions on Systems Science and Cybernetics*, **4**, *3*, 227–241 (1968).
12. D. C. DOWSON and A. WRAGG, "Maximum-Entropy Distributions Having Prescribed First and Second Moments," *IEEE Transactions on Information Theory*, **19**, *5*, 689–693 (1973).
13. J. N. KAPUR, *Maximum-Entropy Models in Science and Engineering*, Wiley (1989).
14. F. H. FRÖHNER, "Assigning Uncertainties to Scientific Data," *Nuclear Science and Engineering*, **126**, *1*, 1–18 (1997).
15. A. TAAVITSAINEN and R. VANHANEN, "On the maximum entropy distributions of inherently positive nuclear data," *Nuclear Instruments and Methods in Physics Research Section A: Accelerators, Spectrometers, Detectors and Associated Equipment* (2016).
16. S. S. WILKS, "Determination of Sample Sizes for Setting Tolerance Limits," *The Annals of Mathematical Statistics*, **12**, *1*, 91–96 (1941).
17. S. S. WILKS, "Statistical Prediction with Special Reference to the Problem of Tolerance Limits," *The Annals of Mathematical Statistics*, **13**, *4*, 400–409 (1942).
18. A. WALD, "An Extension of Wilks' Method for Setting Tolerance Limits," *The Annals of Mathematical Statistics*, **14**, *1*, 45–55 (1943).
19. A. GUBA, M. MAKAI, and L. PÁL, "Statistical aspects of best estimate method – I," *Reliability Engineering & System Safety*, **80**, *3*, 217–232 (2003).
20. G. MARLEAU, A. HÉBERT, and R. ROY, "A user guide for DRAGON version5, IGE-335," Tech. rep., Institut de génie nucléaire, École Polytechnique de Montréal (2014).
21. T. IKONEN ET AL., "Module for thermomechanical modeling of LWR fuel in multiphysics simulations," *Annals of Nuclear Energy*, **84**, 111–121 (2015).
22. T. IKONEN, J. KÄTTÖ, and H. LOUKUSA, "FINIX – Fuel behavior model and interface for multiphysics application – Code documentation for version 0.15.6," Tech. rep., VTT (2015), VTT-R-02988-15.

23. W. J. M. DE KRUIJF, *Reactor Physics Analysis of the Pin-Cell Doppler Effect in a Thermal Nuclear Reactor*, Ph.D. thesis, Delft University of Technology (1994).
24. R. E. MACFARLANE ET AL., *The NJOY Nuclear Data Processing System, Version 2012*, Los Alamos National Laboratory (2012).
25. M. B. CHADWICK ET AL., "ENDF/B-VII.1 Nuclear Data for Science and Technology: Cross Sections, Covariances, Fission Product Yields and Decay Data," *Nuclear Data Sheets*, **112**, *12*, 2887–2996 (2011), Special Issue on ENDF/B-VII.1 Library.
26. R. C. LITTLE ET AL., "Low-fidelity Covariance Project," *Nuclear Data Sheets*, **109**, *12*, 2828–2833 (2008), Special Issue on Workshop on Neutron Cross Section Covariances June 24–28, 2008, Port Jefferson, New York, USA.
27. R. VANHANEN and M. PUSA, "Survey of prediction capabilities of three nuclear data libraries for a PWR application," *Annals of Nuclear Energy*, **83**, 408–421 (2015).
28. E. SARTORI, "OECD/NEA Data Bank: Standard Energy Group Structures of Cross Section Libraries for Reactor Shielding, Reactor Cell and Fusion Neutronics Applications: VITAMIN-J, ECCO-33, ECCO-2000 and XMAS," Tech. rep. (1990), JEF/DOC-315 Revision 3.
29. R. E. MACFARLANE and D. W. MUIR, *The NJOY nuclear data processing system, Version 91*, Los Alamos National Laboratory (1994).
30. M. PUSA, "Incorporating sensitivity and uncertainty analysis to a lattice physics code with application to CASMO-4," *Annals of Nuclear Energy*, **40**, *1*, 153–162 (2012).